Generalized Receiver Designs for OFDM Systems with Alamouti Decoding in Fast Fading Channels

VYACHESLAV TUZLUKOV
Department of Technical Maintenance of Aviation and Radio Electronic Equipment
Belarusian State Aviation Academy
77, Uborevicha Str., 220096 Minsk
BELARUS

Abstract: - In the present paper, the generalized receiver designs for orthogonal frequency-division multiplexing (OFDM) systems that exploit the Alamouti transmit diversity technique are addressed. In Alamouti space-time coded OFDM systems, the simple Alamouti decoding at the generalized receiver relies on the assumption that the channels do not change over an Alamouti codeword period (two consecutive OFDM symbol periods). Unfortunately, when the channel is fast fading, the assumption is not met, resulting in severe performance degradation. In the present paper, a sequential decision feedback sequence estimation (SDFSE) scheme based on the generalized receiver with an adaptive threshold, a traditionally single-carrier equalization technique, is used to mitigate the performance degradation. A new method to set the threshold value is proposed. For small signal constellations like binary phase-shift keying (BPSK) and quadrature phase shift-keying (QPSK), the SDFSE generalized receiver with the adaptive threshold requires much lower complexity than a previous minimum mean square error (MMSE) approach based on the generalized receiver at the cost of small performance degradation. Furthermore, we show that the performance difference becomes smaller when the channel estimation error is included. Adaptive effort sequence estimation (AESE) scheme based on the generalized receiver is also proposed to further reduce the average complexity of the SDFSE generalized receiver scheme with the adaptive threshold. The AESE generalized receiver scheme is based on the observation that a high Doppler frequency does not necessarily mean significant instantaneous channel variations. Simulations demonstrate the efficacy of the proposed SDFSE generalized receiver with the adaptive threshold and AESE generalized receiver schemes.

Key-Words: - Generalized receiver, equalization, orthogonal frequency-division multiplexing (OFDM), sequence estimation, transmit diversity.

1 Introduction

In recent years, transmit diversity techniques have received attention because they increase transmission reliability over wireless fading channels without penalty in bandwidth efficiency [1], [2]. Space-time coding at the transmitter does not require channel state information, thus no feedback from the receiver to the transmitter is necessary [3]-[5]. One popular and practical transmit diversity technique is the Alamouti scheme [6], in which the maximum-likelihood decoding naturally decouples the signals transmitted from different antennas. The simple Alamouti decoding scheme works well when channels are flat fading and time-invariant over the Alamouti codeword period.

Unfortunately, high data rate applications necessitate data transmission over broadband frequency selective channels, which cause severe intersymbol interference. However, a frequency selective channel can be divided into a set of parallel flat fading channels by combining the Alamouti decoding technique with an orthogonal frequency-division multiplexing (OFDM) modulation method. In this Alamouti coded OFDM system, the simple Alamouti decoding at each subchannel requires that channels have to be constant over two OFDM symbol periods. When the quasistatic channel condition is met and an appropriate cyclic prefix is used, the simple Alamouti decoding works well.

The combination of Alamouti technique and OFDM modulation, however, makes the degrading time varying channel effects more severe. Since OFDM systems have much longer symbol duration than single-carrier systems, a channel that is quasistatic for single-carrier systems may not be quasistatic for OFDM systems. Consequently, rapidly changing channels cause more severe performance degradation in the Alamouti coded OFDM systems than in Alamouti coded single-carrier systems. When the channel is fast fading, a channel variation within an

OFDM symbol gives rise to the interchannel interference or coupling between the symbols in different codewords (the intercodeword coupling). In addition, the channel variation between two consecutive OFDM symbols causes coupling between symbols in a codeword at each subchannel (the intracodeword coupling). With two coupling effects lowering the effective signal-to-noise ratio (*SNR*) at the receiver, as will be shown in Section 4.3, the Alamouti decoding performance degradation motivates the need for a decoding scheme that improves the performance at moderate complexity.

The effect of a fast fading channel on the bit-error rate (*BER*) performance of OFDM systems was analyzed in [10], however, no transmit diversity technique was considered in [10]. Performance degradation due to fast fading channels in systems with transmit diversity using the Alamouti code was considered in [11]. Since a single-carrier system was considered in [11], however, the interchannel interference was not included as a performance degrading factor. In [12], a new model of signal-to-interference plus noise ratio (*SINR*) in a multiple-input multiple-output (MIMO) OFDM system, including the impact of time-varying channels was proposed. In the present paper, we separate the impact of the time-varying channel into the intercodeword and intracodeword couplings (both are defined in Section 4.2) and use them to analyze the effect of channel variation within an OFDM symbol period.

Various decoding schemes for space-time coded systems have been proposed. In [13], it was reported that transmit diversity exploiting the Alamouti code and its simple decoding can be used for a single-carrier system even when channels are not quasistatic. This is possible due to in part to a relatively short symbol period of single-carrier systems when compared with OFDM systems. In [14] a simplified maximum likelihood (ML) decoder for a space-time block-coded single-carrier system was proposed when channels are time selective. A decoding matrix was proposed in an effort to make the resultant matrix (channel matrix multiplied by the decoding matrix) diagonal, eliminating interantenna interference. An adaptive frequency domain equalization scheme was also proposed for single-carrier systems in [15] to track channel variations within a transmission block. The previous approaches [13]-[15] consider single-carrier systems, where the interchannel interference is not applicable, thus these approaches do not apply to OFDM systems.

Decoding schemes in OFDM systems with transmit diversity were reported in [12], [16], and [17]. A time-domain filtering approach was proposed in [12] for MIMO OFDM systems in the fast fading channels. We compare our proposed approaches mainly with this previous approach. In [12], a time-variant filter has been designed in the time domain so that *SINR* including a channel variation effect is maximized. As will be shown in detail later, however, the design process as well as the filtering process is computationally expensive for some system parameters. In [16], a space-frequency encoding/decoding scheme for wideband OFDM system was proposed to improve performance, concatenating space-time block coding with trellis coded modulation (thereby increasing complexity). However, a slow fading channel is assumed in [16], which is not the case we consider in the present paper. OFDM systems with the interchannel interference and intersymbol interference were considered in [17] and a decision feedback equalization structured equalizer was designed. However, the interchannel interference considered in [17] is due to insufficient cyclic prefix length rather than fast fading channels.

A differential space-time block coding scheme was developed based on the Alamouti scheme in [18], eliminating the need for channel estimation. The differential scheme becomes relatively more bandwidth efficient, when compared with a coherent scheme, in the fast fading channels because no training symbols is required to estimate the channels. The differential scheme, however, assumes that the channels do not change over two Alamouti codeword periods, which is not true under the fast fading channels under consideration. Therefore, the fast time variation of the channels is likely to have a more severe impact on performance of differentially space-time block coded systems than on coherent systems We compare the performance of the proposed generalized receivers with the differentially coded system through simulations at a high Doppler frequency and demonstrate the advantages of coherent approaches in Section 6. Although a more thorough comparison could be made considering the different Doppler frequencies at the different channel state information estimation schemes, we consider only the fixed high Doppler frequency and one channel state information scheme.

In the present paper, we analyze the intercodeword and intracodeword coupling effects and demonstrate their severity via simulation. Then, we use sequence estimation schemes [19]-[25] that are traditionally single-carrier equalization techniques to alleviate the performance degradation due to the coupling effects. Firstly, we formulate the maximum likelihood sequence estimation (MLSE) scheme based on the generalized receiver in the frequency domain. In [26], it was argued that small normalized Doppler frequency, the product of the Doppler frequen-

cy and symbol period, implies that the interchannel interference is from only a few nearest subchannels. In the MLSE formulation, we take an advantage of an observation that even when the normalized Doppler frequency is somewhat large, we need to compensate for the interchannel interference from only a few nearest subchannels because of the channel estimation error as well as less significance of the interchannel interference from far away subchannels. Secondly, a sequential decision feedback sequence estimation (SDFSE) scheme based on the generalized receiver with the adaptive threshold is described as a suboptimal scheme that reduces the high computational complexity of the maximum likelihood sequence estimation. The complexity of the SDFSE generalized receiver scheme is again reduced by using the adaptive threshold. Twice the intercodeword coupling, which will be defined later, is used as a threshold value. The SDFSE generalized receiver scheme with the adaptive threshold is composed of candidate selection step and sequence estimation step. The applicability of the adaptive threshold idea is based on the observation that the intercodeword coupling is much weaker than the intracodeword coupling. The relatively small intercodeword coupling keeps the number of candidates small to make efficient the SDFSE generalized receiver scheme with the adaptive threshold.

To further reduce the average complexity of the SDFSE generalized receiver scheme with the adaptive threshold, we propose an adaptive effort symbol estimation (AESE) scheme based on the generalized receiver. Basically, the simple Alamouti decoding scheme is selected when the instantaneous channel variation is negligible, and the SDFSE generalized receiver scheme with the adaptive threshold is used when the channel variation is significant. The degree of the channel variation is measured in terms of the intracodeword coupling, which is defined later. When the intracodeword coupling is larger than a certain threshold, instantaneous channel parameter variation is considered as significant, and vice versa. The threshold value in the AESE generalized receiver scheme is set from simulation experiments. The AESE generalized receiver scheme is motivated by observation that the high Doppler frequency does not necessarily mean the instantaneous significant channel variation. Therefore, even when the Doppler frequency is very high, the transmitted symbols are estimated via the Alamouti decoding when the instantaneous channel variation is negligible. The Alamouti decoding, the SDFSE scheme with the adaptive threshold, AESE scheme, and the time-domain MMSE approach (all of them are constructed based on the generalized receiver) are compared in

terms of complexity and performance via simulation Since each signal estimation scheme may react differently to channel estimation error, we consider both cases with and without the ideal channel state information. We use the channel estimation technique involving pilot tone and interpolation in [12] to estimate the channel state information. All proposed schemes, namely, SDFSE, AESE, MMSE, MLSE, discussed in the present paper are based on the generalized approach to signal processing in noise (see Section 3) [27]-[29].

The remainder of this paper is organized as follows. In Section 2, the Alamouti coded OFDM system with two transmit antennas and one receive antenna is described. In Section 3, the main functioning principles of the generalized receiver constructed based on the generalized approach to signal processing in noise are discussed. In Section 4, the Alamouti decoding scheme is investigated under both quasistatic and fast fading channel environments. The relative significance of the two coupling effects and consequent performance degradation are both analyzed and demonstrated via simulation. In Section 5, symbol estimation schemes in the fast fading channels are described. In Section 6, computer simulation experiments are conducted to compare the performance of the schemes characterized by different levels of complexity. Conclusions are presented in Section 7.

In the present paper, a boldface letter denotes the vector or matrix, as will be clear from the context; $\mathbf{I}_M$ denotes the $M \times M$ identity matrix; $(\cdot)^*$ denotes the complex conjugate; $(\cdot)^T$ denotes the transpose; $(\cdot)^H$ denotes the Hermitian transpose; $|\cdot|$ denotes the absolute value; $\|\cdot\|$ denotes the L_2 norm of matrix or vector; in general, a lowercase letter stands for the time-domain signal while an uppercase letter denotes frequency domain signal. If $\sigma \cong (a,b,\ldots,z)$ is a sequence, $\sigma \setminus a = (b,c,\ldots,z)$. The notation $(\mathbf{X}[m] \mid m \in \mathcal{K})$, where $\mathcal{K}$ is the set, denotes a sequence whose elements indexes are increasingly ordered.

2 System Model

In the present paper, we consider an OFDM system with transmit diversity as illustrated in Fig.1. The bandwidth $B = 1/T_s$, where T_s is the sampling interval, is divided into N equally spaced subcarriers at frequencies $k\Delta f, k = 0,1,\ldots,N-1$ with $\Delta f = B/N$. At the transmitter, information bits are grouped and mapped into complex symbols. In the present paper, quadrature phase shift-keying (QPSK) with constel-

lation C_{QPSK} is assumed for the symbol mapping. According to the Alamouti code, $\{X_1[k]\ X_2[k]\}$ are transmitted by two antennas simultaneously during the first symbol period $(l=1)$ for each $k\in\mathcal{K}$. During the second symbol period $(l=2)$, $\{-X_2^*[k]\ X_1^*[k]\}$ are transmitted by two antennas for each $k\in\mathcal{K}$. The set

$$\mathcal{K}\cong\{(N-N_c/2),\ldots,(N+N_c/2)-1\}\qquad(1)$$

is the set of data carrying subcarrier indexes, and N_c is the number of subcarriers carrying data; N is the fast Fourier transform (FFT) size; consequently, the number of virtual carriers is $N-N_c$. We assume half
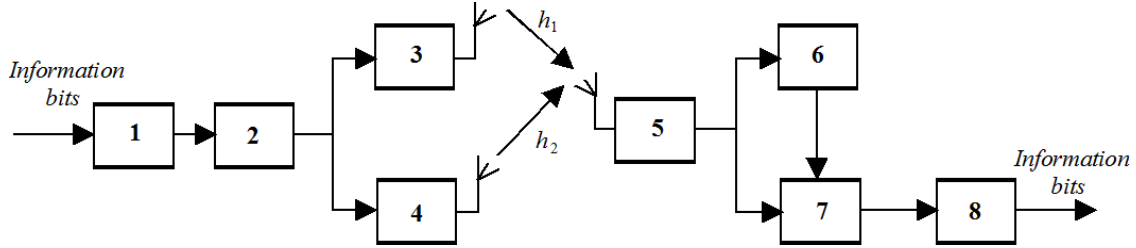

Fig.1. OFDM system with transmit diversity: 1- QPSK modulator; 2 – STBC encoder; 3,4 – inverse fast Fourier transform; 5 – fast Fourier transform; 6 – channel estimation; 7 – space-time decoder; 8 – QPSK demodulator

of the virtual carriers are on both ends of the spectral band. The inverse FFT (IFFT) converts each $N\times1$ complex vector into a time-domain signal and the copy of the last D samples is appended as a cyclic prefix. Thus, the length of an OFDM symbol is $(N+D)T_s$. The time-domain signals transmitted by the antenna i during the lth symbol period $x_{i,l}[n],0\leq n\leq N+D-1$, $i\in\{1,2\}$, $l\in\{1,2\}$ are expressed as

$$x_{i,l}[n]=\sum_{k\in\mathcal{K}}S_{i,l}[k]\exp\{j2\pi k(n-D)/N\}\ ,\qquad(2)$$

where $S_{i,l}[k]$ denotes the complex symbol transmitted by the i-th antenna during the l-th symbol period in the Alamouti codeword over the k-th subchannel. The index for the Alamouti codeword is omitted to keep the notation simple.

The signals from the two transmitting antennas go through independent channels. The wireless channel can be described as L resolved multipath components $p\in\{0,1,\ldots,L-1\}$, each characterized by the amplitude $h_{i,l}[n,p]$ and delay pT_s, where $h_{i,l}[n,p]$ stands for the p-th resolved multipath component amplitude between the i-th transmit antenna and the receive antenna at the time n (the sample index) during the l-th symbol period. The maximum delay spread of the two channels is assumed to be the same and equals to $(L-1)T_s$.

The received signals during the Alamouti codeword period take the following form

$$y_l[n]=\sum_{i=1}^{2}\sum_{p=0}^{L-1}h_{i,l}[n,p]x_{i,l}[n-p]+w_l[n]\ ,\ l\in\{1,2\},$$

$$(3)$$

where $w_l[n]$ is the circularly symmetric zero-mean white complex Gaussian random process. It can be observed that the received signals are the superposition of signals generated by two transmitting antennas. If the cyclic prefix length D is longer than $L-1$ the received signals given by (3) after removing the prefix can be considered as the circular convolution result of the transmitted signal given by (2) and the channel. Consequently, the demodulated signals in the frequency domain via the FFT are expressed as

$$Y_l[k]=\sum_{i=1}^{2}\sum_{m\in\mathcal{K}}S_{i,l}[m]a_{i,l}[k,m]+W_l[k]\ ,\ l\in\{1,2\}\quad(4)$$

where

$$a_{i,l}[k,m]\cong\sum_{p=0}^{L-1}H_{i,l,p}[k-m]\exp\{-j2\pi mp/N\}\ ;\quad(5)$$

$$H_{i,l,p}[k-m]\cong\frac{1}{N}\sum_{n=0}^{N-1}h_{i,l}[n,p]\exp\{-j2\pi(k-m)n/N\}$$

$$(6)$$

The notation $H_{i,l,p}[k-m]$ represents the FFT of the p-th multipath component between the i-th transmitting antenna and the receive antenna during the l-th symbol period. Note that $a_{i,l}[k,m],m\neq k$ denotes

the interchannel interference from the *m*-th subchannel to the *k*-th subchannel for each transmit antenna index $i \in \{1,2\}$ and symbol period $l \in \{1,2\}$. An additional interpretation of $H_{i,l,p}[k-m]$ and $a_{i,l}[k,m]$ is provided in [26].

3 Generalized Receiver: Main Functioning Principles

The generalized receiver is constructed in accordance with the generalized approach to signal processing in noise [27]-[29]. The generalized approach to signal processing in noise introduces an additional noise source that does not carry any information about the parameters of desired transmitted signal with the purpose to improve the signal processing system performance. This additional noise can be considered as the reference noise without any information about the parameters of the signal to be detected.

The jointly sufficient statistics of the mean and variance of the likelihood function is obtained under the generalized approach to signal processing in noise employment, while the classical and modern signal processing theories can deliver only the sufficient statistics of the mean or variance of the likelihood function. Thus, the generalized approach to signal processing in noise implementation allows us to obtain more information about the parameters of the desired transmitted signal incoming at the generalized receiver input. Owing to this fact, the detectors constructed based on the generalized approach to signal processing in noise technology are able to improve the signal detection performance of signal processing systems in comparison with employment of other conventional detectors.

The generalized receiver (GR) consists of three channels (see Fig. 2): the GR correlation detector channel (GR CD) – the preliminary filter (PF), the multipliers 1 and 2, the model signal generator (MSG); the GR energy detector channel (GR ED) – the PF, the additional filter (AF), the multipliers 3 and 4, the summator 1; and the GR compensation channel (GR CC) – the summators 2 and 3, the accumulator 1. The threshold apparatus (THRA) device defines the GR threshold.

As we can see from Fig.2, there are two bandpass filters, i.e., the linear systems, at the GR input, namely, the PF and AF. We assume for simplicity that these two filters or linear systems have the same amplitude-frequency characteristics or impulse responses. The AF central frequency is detuned relative to the PF central frequency.

There is a need to note the PF bandwidth is matched with the transmitted signal bandwidth. If the

detuning value between the PF and AF central frequencies is more than 4 or 5 times the transmitted signal bandwidth to be detected, i.e., $4 \div 5 \Delta f_s$, where Δf_s is the transmitted signal bandwidth, we can believe that the processes at the PF and AF outputs are uncorrelated because the coefficient of correlation between them is negligible (not more than 0.05). This fact was confirmed experimentally in [30] and [31] independently. Thus, the transmitted signal plus noise can be appeared at the GR PF output and the noise only is appeared at the GR AF output. The stochastic processes at the GR AF and GR PF outputs present the input stochastic samples from two independent frequency-time regions. If the discrete-time noise $w_i[k]$ at the GR PF and GR AF inputs is Gaussian, the discrete-time noise $\zeta_i[k]$ at the GR PF output is Gaussian too, and the reference discrete-time noise $\eta_i[k]$ at the GR AF output is Gaussian owing to the fact that the GR PF and GR AF are the linear systems and we believe that these linear systems do not change the statistical parameters of the input process. Thus, the GR AF can be considered as a generator of the reference noise with a priori information a "no" transmitted signal (the reference noise sample) [28, Chapter 5]. The noise at the GR PF and GR AF outputs can be presented as

$$
\begin{cases}
\zeta_i[k] = \displaystyle\sum_{m=-\infty}^{\infty} g_{PF}[m] w_i[k-m] \; ; \\
\eta_i[k] = \displaystyle\sum_{m=-\infty}^{\infty} g_{AF}[m] w_i[k-m] \; ,
\end{cases}
\tag{7}
$$

where $g_{PF}[m]$ and $g_{AF}[m]$ are the impulse responses of the GR PF and GR AF, respectively.

In a general, under practical implementation of any detector in wireless communication system with sensor array, the bandwidth of the spectrum to be sensed is defined. Thus, the GR AF bandwidth and central frequency can be assigned, too (this bandwidth cannot be used by the transmitted signal because it is out of its spectrum). The case when there are interfering signals within the GR AF bandwidth, the action of this interference on the GR detection performance, and the case of non-ideal condition when the noise at the GR PF and GR AF outputs is not the same by statistical parameters are discussed in [32] and [33].

Under the hypothesis $\mathcal{H}_1$ ("a yes" transmitted signal), the GR CD generates the signal component $s_i^m[k] s_i[k]$ caused by interaction between the model signal $s_i^m[k]$, forming at the MSG output, and the incoming signal $s_i[k]$, and the noise component $s_i^m[k]$

$\times \zeta_i[k]$ caused by interaction between the model signal $s_i^m[k]$ and the noise $\zeta_i[k]$ at the PF output. GR ED generates the transmitted signal energy $s_i^2[k]$ and the random component $s_i[k]\zeta_i[k]$ caused by interaction between the transmitted signal $s_i[k]$ and the noise $\zeta_i[k]$ at the PF output. The main purpose of the GR CC is to cancel completely in the statistical sense the GR CD noise component $s_i^m[k]\zeta_i[k]$ and the

GR ED random component $s_i[k]\zeta_i[k]$ based on the same nature of the noise $\zeta_i[k]$. The relation between the transmitted signal to be detected $s_i[k]$ and the model signal $s_i^m[k]$ is defined as:

$$s_i^m[k] = \mu\, s_i[k] \ , \tag{8}$$

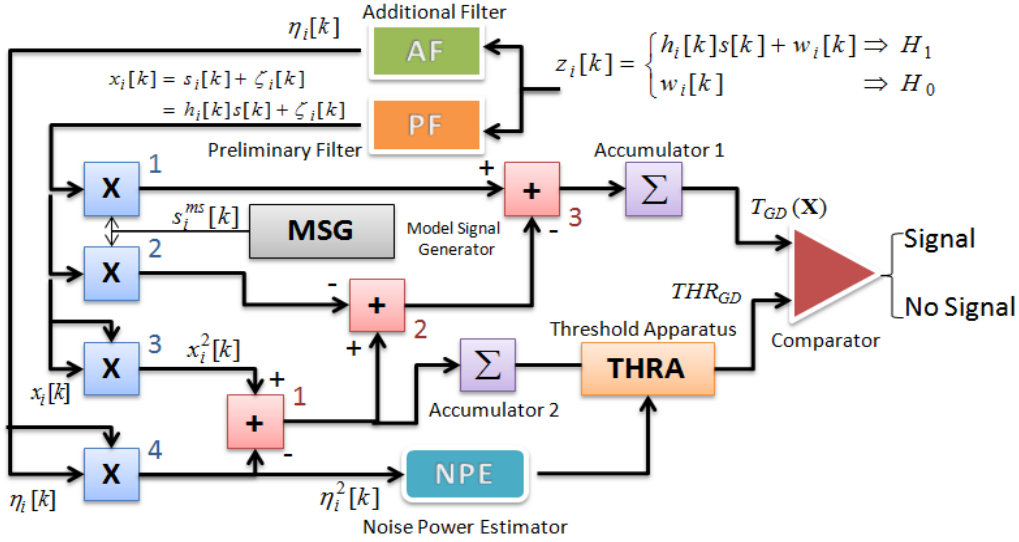where μ is the coefficient of proportionality.

Fig. 2. Generalized receiver.

The main functioning condition under the GR employment in any signal processing system including the communication one with radar sensors is the equality between the parameters of the model signal $s_i^m[k]$ and the incoming signal $s_i[k]$, for example, by amplitude. Under this condition it is possible to cancel completely in the statistical sense the noise component $s_i^m[k]\zeta_i[k]$ of the GR CD and the random component $s_i[k]\zeta_i[k]$ of the GR ED. Satisfying the GR main functioning condition given by (8), $s_i^m[k] = s_i[k]$, $\mu = 1$, we are able to detect the transmitted signal with the high probability of detection at the low *SNR* and define the transmitted signal parameters with the required high accuracy.

Practical realization of the condition (8) at $\mu \to 1$ requires increasing in the complexity of GR structure and, consequently, leads us to increasing in computation cost. For example, there is a need to employ the amplitude tracking system or to use the offline data samples processing. Under the hypothesis $\mathcal{H}_0$ ("a no" transmitted signal), satisfying the main GR functioning condition (8) at $\mu \to 1$ we obtain on-

ly the background noise $\eta_i^2[k] - \zeta_i^2[k]$ at the GR output.

Under practical implementation, the real structure of GR depends on specificity of signal processing systems and their applications, for example, the radar sensor systems, adaptive wireless communication systems, cognitive radio systems, satellite communication systems, mobile communication systems and so on. In the present paper, the GR circuitry (Fig.2) is demonstrated with the purpose to explain the main functioning principles. Because of this, the GR flowchart presented in the paper should be considered under this viewpoint. Satisfying the GR main functioning condition (8) at $\mu \to 1$, the ideal case, for the wireless communication systems with radar sensor applications we are able to detect the transmitted signal with very high probability of detection and define accurately its parameters.

In the present paper, we discuss the GR implementation in the broadband space-time spreading MC DS-CDMA wireless communication system. Since the presented GR test statistics is defined by the signal energy and noise power, the equality between the parameters of the model signal $s_i^m[k]$ and trans-

mitted signal to be detected $s_i[k]$, in particular by amplitude, is required that leads us to high circuitry complexity in practice.

For example, there is a need to employ the amplitude tracking system or off-line data sample processing. Detailed discussion about the main GR functioning principles if there is no a priori information and there is an uncertainty about the parameters of transmitted signal, i.e., the transmitted signal parameters are random, can be found in [27], [28, Chapter 6, pp.611–621 and Chapter 7, pp. 631–695].

The complete matching between the model signal $s_i^m[k]$ and the incoming signal $s_i[k]$, for example by amplitude, is a very hard problem in practice because the incoming signal $s_i[k]$ depends on both the fading and the transmitted signal parameters and it is impractical to estimate the fading gain at the low *SNR*. This matching is possible in the ideal case only. The GD detection performance will be deteriorated under mismatching in parameters between the model signal $s_i^m[k]$ and the transmitted signal $s_i[k]$ and the impact of this problem is discussed in [34]-[37], where a complete analysis about the violation of the main GR functioning requirements is presented. The GR decision statistics requires an estimation of the noise variance σ_η^2 using the reference noise $\eta_i[k]$ at the AF output.

Under the hypothesis $\mathcal{H}_1$, the signal at the GR PF output, see Fig. 2, can be defined as

$$x_i[k] = s_i[k] + \zeta_i[k] \ , \qquad (9)$$

where $\zeta_i[k]$ is the noise at the PF output and

$$s_i[k] = h_i[k]s[k], \qquad (10)$$

where $h_i[k]$ are the channel coefficients. Under the hypothesis $\mathcal{H}_0$ and for all i and k, the process $x_i[k] = \zeta_i[k]$ at the PF output is subjected to the complex Gaussian distribution law and can be considered as the i.i.d. process.

In the ideal case, we can think that the signal at the GR AF output is the reference noise $\eta_i[k]$ with the same statistical parameters as the noise $\zeta_i[k]$. In practice, there is a difference between the statistical parameters of the noise $\eta_i[k]$ and $\zeta_i[k]$. How this difference impacts on the GR detection performance is discussed in detail in [28, Chapter 7, pp. 631-695] and in [34]-[37],

The decision statistics at the GR output presented in [30] and [31, Chapter 3] is extended for the case of antenna array when an adoption of multiple antennas and antenna arrays is effective to mitigate the

negative attenuation and fading effects. The GR decision statistics can be presented in the following form:

$$T_{GR}(\mathbf{X}) = \sum_{k=0}^{N-1}\sum_{i=1}^{M} 2x_i[k]s_i^m[k]$$

$$-\sum_{k=0}^{N-1}\sum_{i=1}^{M} x_i^2[k] + \sum_{k=0}^{N-1}\sum_{i=1}^{M} \eta_i^2[k] \overset{\mathcal{H}_1}{\underset{\mathcal{H}_0}{\gtrless}} THR_{GR} \ , \quad (11)$$

where

$$\mathbf{X} = \left[\mathbf{x}(0),...,\mathbf{x}(N-1)\right] \qquad (12)$$

is the vector of the random process at the GR PF output and THR_{GR} is the GR detection threshold.

Under the hypotheses $\mathcal{H}_1$ and $\mathcal{H}_0$ when the amplitude of the transmitted signal is equal to the amplitude of the model signal, $s_i^m[k] = s_i[k]$, $\mu = 1$, the GR decision statistics $T_{GD}(\mathbf{X})$ takes the following form in the statistical sense, respectively:

$$\begin{cases} \mathcal{H}_1 : T_{GD}(\mathbf{X}) = \sum_{k=0}^{N-1}\sum_{i=1}^{M}\{s_i^2[k] + \eta_i^2[k] - \zeta_i^2[k]\} \\ \\ \mathcal{H}_0 : T_{GD}(\mathbf{X}) = \sum_{k=0}^{N-1}\sum_{i=1}^{M}\{\eta_i^2[k] - \zeta_i^2[k]\} \end{cases} . \quad (13)$$

In (13) the term $\sum_{k=0}^{N-1}\sum_{i=1}^{M} s_i^2[k] = E_s$ corresponds to the average transmitted signal energy, and the term $\sum_{k=0}^{N-1}\sum_{i=1}^{M}\eta_i^2[k] - \sum_{k=0}^{N-1}\sum_{i=1}^{M}\zeta_i^2[k]$ is the background noise at the GR output. The GR output background noise is the difference between the noise power at the GR PF and GR AF outputs. Practical implementation of the GR decision statistics requires an estimation of the noise variance σ_η^2 using the reference noise $\eta_i[k]$ at the AF output.

4 Alamouti Decoding Scheme

In this section, the Alamouti decoding scheme is briefly reviewed under assumption of quasistatic channel. Then, the performance degradation of the scheme in a fast fading channel is both analyzed and demonstrated via computer simulations.

4.1 Slow fading channel

If the channel is slow fading, the interchannel interference terms are not significant as described in [8] and

$$a_{i,l}[k,m] \approx 0 \quad \forall m \neq k \ . \qquad (14)$$

As a result, the received signal given by (4) is expressed as a set of simultaneous equations

$$\mathbf{Y}[k] = \mathbf{A}[k,k]\mathbf{X}[k] + \mathbf{W}[k], \quad k \in \mathcal{K} \quad (15)$$

where

$$\mathbf{A}[k,m] \cong \begin{bmatrix} a_{1,1}[k,m] & a_{2,1}[k,m] \\ a_{2,2}^*[k,m] & -a_{1,2}^*[k,m] \end{bmatrix} \text{ for } k,m \in \mathcal{K} ; \quad (16)$$

$$\begin{cases} \mathbf{Y}[k] \cong \begin{bmatrix} Y_1[k] & Y_2^*[k] \end{bmatrix}^T ; \\ \mathbf{X}[k] \cong \begin{bmatrix} X_1[k] & X_2^*[k] \end{bmatrix}^T ; \\ \mathbf{W}[k] \cong \begin{bmatrix} W_1[k] & W_2^*[k] \end{bmatrix}^T . \end{cases} \quad (17)$$

Via the assumption that the channels do not change over an Alamouti codeword period, i.e.,

$$\begin{cases} a_{1,1}[k,k] = a_{1,2}[k,k] = \alpha_1[k], \\ a_{2,1}[k,k] = a_{2,2}[k,k] = \alpha_2[k], \end{cases} \quad (18)$$

space-time decoding is performed by multiplying both sides of (15) with $\mathbf{A}^H[k,k]$ to estimate the transmitted symbols

$$\tilde{\mathbf{X}}[k] = (|\alpha_1[k]|^2 + |\alpha_2[k]|^2)\mathbf{X}[k] + \mathbf{A}^H[k,k]\mathbf{W}[k]. \quad (19)$$

Note that two symbols in $\tilde{\mathbf{X}}[k]$ are decoupled from each other. The final decisions are made independently

$$\hat{X}_i[k] = \operatorname{argmin}_{X \in C_{QPSK}} \| \tilde{X}_i[k] - \rho[k]X[k] \| , \ i \in \{1,2\} \quad (20)$$

with

$$\rho[k] \cong |\alpha_1[k]|^2 + |\alpha_2[k]|^2 . \quad (21)$$

4.2 Fast fading channel

When the channel is fast fading, however, approximation (14) is not more valid and the received signal (4) is split into N_c equations as follows

$$\mathbf{Y}[k] = \mathbf{A}[k,k]\mathbf{X}[k] + \sum_{\substack{m \in \mathcal{K} \\ m \neq k}} \mathbf{A}[k,m]\mathbf{X}[m] + \mathbf{W}[k], k \in \mathcal{K} \quad (22)$$

If we define

$$\tilde{\mathbf{A}}[k] \cong \begin{bmatrix} \alpha_1[k] & \alpha_2[k] \\ \alpha_2^*[k] & -\alpha_1^*[k] \end{bmatrix} , \quad (23)$$

where

$$\alpha_1[k] = a_{1,1}[k,k] \text{ and } \alpha_2[k] = a_{2,1}[k,k] , \quad (24)$$

then

$$\tilde{\mathbf{A}}[k]\mathbf{A}[k] = \rho[k]\mathbf{I}_2 , \quad (25)$$

where $\mathbf{I}_2$ is the unit matrix with the size 2×2.

The following equation can be derived from (22) using the above identity

$$\tilde{\mathbf{Y}}[k] = \rho[k]\mathbf{X}[k] + \mathbf{C}_{INTRA}[k]\mathbf{X}[k] + \sum_{\substack{m \in \mathcal{K} \\ m \neq k}} \mathbf{C}_{INTER}[k,m]\mathbf{X}[m] + \tilde{\mathbf{W}}[k] , \ k \in \mathcal{K} \quad (26)$$

where

$$\begin{cases} \tilde{\mathbf{Y}}[k] \cong \tilde{\mathbf{A}}^H[k]\mathbf{Y}[k]; \\ \mathbf{C}_{INTRA}[k] \cong \tilde{\mathbf{A}}^H[k]\mathbf{A}_\Delta[k]; \\ \mathbf{C}_{INTER}[k,m] \cong \tilde{\mathbf{A}}^H[k]\mathbf{A}[k,m]; \\ \tilde{\mathbf{W}}[k] \cong \tilde{\mathbf{A}}^H[k]\mathbf{W}[k]; \\ \mathbf{A}_\Delta[k] \cong \mathbf{A}[k,k] - \tilde{\mathbf{A}}[k]. \end{cases} \quad (27)$$

It can be observed that the second and third terms on the right side of (26) show the effect of the time-variant channel. The second term shows the coupling effect between symbols in the codeword (the intracodeword coupling) and the third term shows the coupling effect between symbols in the different codewords (the intercodeword coupling) or the interchannel interference. These two coupling effects create the interference that is lower than the effective *SNR* at each subchannel, thereby degrading the performance [38].

To show the relative significance of the two coupling effects, the following two statistics and the coupling function are defined as

$$\overline{C}_{INTRA}[k] \cong \frac{1}{N_c} \sum_{k \in \mathcal{K}} E[\| \mathbf{C}_{INTRA}[k] \|^2] ; \quad (28)$$

$$\overline{C}_{INTER}[k_0] \cong \frac{1}{N_c} \sum_{k \in \mathcal{K}} E[\| \mathbf{C}_{INTER}[k,k+k_0] \|^2] ; \quad (29)$$

$$\mathbf{\Psi}[k,k_0] \cong \begin{cases} \mathbf{C}_{INTRA}[k], & \text{if } k_0 = 0 \\ \mathbf{C}_{INTER}[k,k+k_0], & \text{otherwise,} \end{cases} \quad (30)$$

where $E[\cdot]$ is the mathematical expectation. From (28)-(30), the following statistic is obtained

$$\overline{\mathbf{\Psi}}[k_0] \cong \frac{1}{N_c} \sum_{k \in \mathcal{K}} E[\| \mathbf{\Psi}[k,k_0] \|^2]$$

$$= \begin{cases} \overline{C}_{INTRA}[k], & \text{if} \quad k_0 = 0 \\ \overline{C}_{INTER}[k_0], & \text{otherwise.} \end{cases} \quad (31)$$

The statistic $\overline{\Psi}[0]$ shows the average intracodeword coupling degree. When $k_0 \neq 0$, $\overline{\Psi}[k_0]$ is the average intercodeword coupling amount from a subchannel that is k_0 times the subcarrier spacing away from an observed subchannel.

4.3 Numerical examples

In this section, the two coupling effects and performance degradation due to the coupling effects are demonstrated via simulation. A two transmitting antenna and one receive antenna OFDM system is simulated. Exact channel estimation at the receiver is assumed. The bandwidth is $B = 400$ kHz, the FFT size $N = 128$, the cyclic prefix length $D = 32$, and the number of data carrying subchannels $N_c = 120$; consequently, the number of virtual carriers is $N - N_c = 8$, and the OFDM symbol period $(N + D)T_s = 400$ μs. Four subchannels on both ends of the spectrum are not used for data transmission. Each subcarrier is modulated by QPSK symbols. The performance criterion is the *BER* versus *SNR* at the receiver input. The total signal power from two transmitting antennas is used for the calculation of the *SNR*. The mobile channel used for simulation is a two-path channel with equal power and delays of zero and $4T_s$, respectively, with each path experiencing independent Rayleigh fading. Jakes' model was used for the Rayleigh fading channel simulation [39]. Doppler frequency considered is 297 Hz, which results in more severe channel variation than the scenario in [12]. For the statistic (31) and the *BER* measurement, 1000 OFDM symbols (500 Alamouti codewords) are transmitted and estimated.

Figure 3 demonstrates an empirical $\overline{\Psi}[k_0]/\overline{\Psi}[0]$, $k_0 \in \{0, \pm 1, \ldots, \pm 10\}$ when $f_D = 297$ Hz. The simulation result suggests that the intracodeword coupling is much stronger than the intercodeword coupling. Figure 4 displays the *BER* as a function of *SNR* at the receiver input for Doppler frequencies of 50 and 297 Hz and demonstrates the performance degradation in the fast fading channels when the standard Alamouti decoding scheme is used. As the Doppler frequency increases from 50 to 297 Hz, the error performance is degraded significantly, especially at the high *SNR*, i.e., *SNR* >15 dB. Given the relative significance of the two coupling effects in Fig. 3, it can be said that the performance degradation is mainly due to the intracodeword coupling effect rather then

the intercodeword coupling effect. The performance degradation motivates a novel symbol estimation scheme, which compensates for the coupling effects at a moderate complexity. In the next section, symbol estimation schemes are described that improve the performance under the fast fading channel environment.
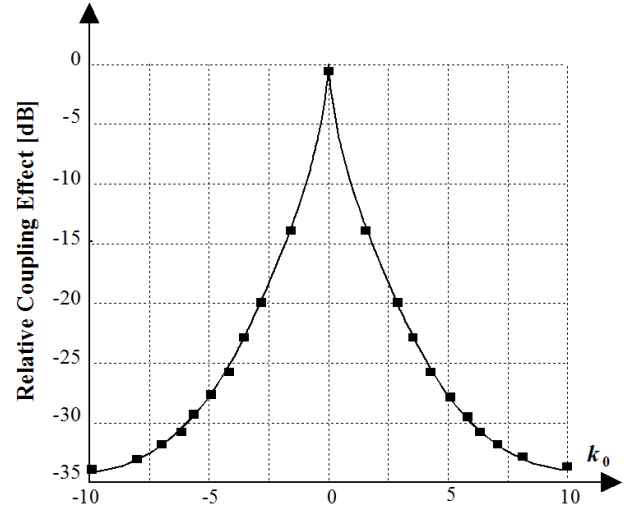

Fig. 3. Relative significance of the couplings caused by the time-variant channel $10\lg(\overline{\Psi}[k_0]/\overline{\Psi}[0])$ versus k_0, at $f_D = 297$ Hz
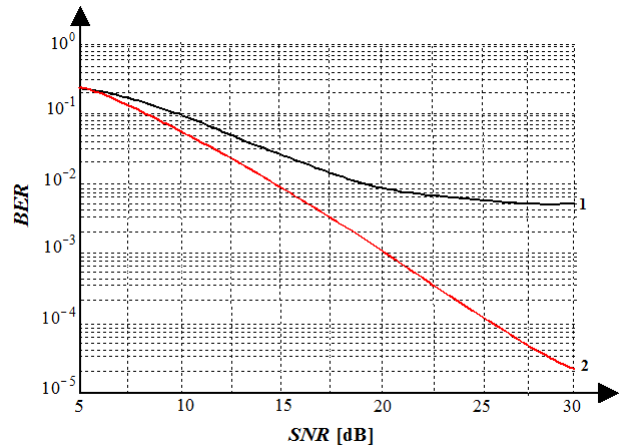

Fig. 4. *BER* performance versus *SNR* of the Alamouti decoding scheme: 1- $f_D = 297$ Hz; 2 - $f_D = 50$ Hz.

5 Symbol Estimation under Fast Fading Channel Environment

In this section, symbol estimation schemes are described in the presence of the coupling discussed in Section 4.2. In Section 5.1, the MLSE generalized receiver approach is formulated for the system under consideration. In Section 5.2, the SDFSE generalized receiver scheme with the adaptive threshold is

described as the suboptimal scheme reducing the complexity of the MLSE generalized receiver approach. Section 5.3 describes the AESE generalized receiver scheme. Section 5.4 considers the required computational complexity, especially compared with the MMSE generalized receiver approach.

5.1 MLSE formulation

In this section, the MLSE generalized receiver scheme is formulated. In the present paper, the Alamouti coded OFDM system is considered, while a trellis-based space-time code was considered in [7] and [9]. When the channel is the fast fading, the two coupling effects described in Section 4.2 need to be compensated. It was argued that if the normalized Doppler frequency is small, we can assume that interchannel interference is from only a few nearest subchannels [26]. We argue that even when the normalized Doppler frequency is pretty large, we have only to consider the interchannel interference from a few nearest subchannels due to channel estimation error as well as less significance of interchannel interference from far away subchannels. By this assumption, the received signal (22) is simplified into

$$\mathbf{Y}[k] = \mathbf{A}[k,k]\mathbf{X}[k]$$
$$+ \sum_{m=\max[k-q,(N-N_c)/2],m\neq k}^{\min[k+q,(N+N_c)/2-1]} \mathbf{A}[k,m]\mathbf{X}[m] + \mathbf{W}[k], \quad (32)$$

where $2q$ is the number of subchannels considered as the causing intercodeword couplings.

It can be observed in (32) that the received signal is composed of the attenuated desired signal, interchannel interference from $2q$ other subchannel, and the additive noise.

Let

$$P(\mathbf{Y}_l, l \in \{1,2\} \mid \mathbf{X}_i = \hat{\mathbf{X}}_i, i \in \{1,2\}) \quad (33)$$

is the conditional probability that $\mathbf{Y}_l, l \in \{1,2\}$ are received under assumption that the $\hat{\mathbf{X}}_i, i \in \{1,2\}$ are transmitted. In the MLSE generalized receiver scheme, we estimate the transmitted sequence to be the sequence that maximizes the likelihood in (33). Since $\mathbf{W}[k]$ in (32) is the white complex Gaussian random process, we can show that the MLSE generalized receiver scheme amounts to computing [19]

$$(\hat{\mathbf{X}}[m] \mid m \in \mathcal{K}) = \operatorname*{argmin}_{(\hat{\mathbf{X}}[m]\mid m\in\mathcal{K})} \sum_{k\in\mathcal{K}} \xi_{MLSE}[k] \quad, \quad (34)$$

where

$$\xi_{MLSE}[k] = \left\| \mathbf{Y}(k) - \sum_{m=\max[k-q,(N-N_c)/2],m\neq k}^{\min[k+q,(N+N_c)/2-1]} \mathbf{A}[k,m]\mathbf{X}[m] \right\| . (35)$$

After a simple modification of the coupling function (30), the following function is defined

$$\mathbf{\Psi}_{imp}[k,k_0] \cong \begin{cases} \rho[k]\mathbf{I}_2 + \mathbf{\Psi}[k,k_0], & \text{if } k_0 = 0 \\ \mathbf{\Psi}[k,k_0], & \text{if } k_0 \in \{\pm1,\pm2,\ldots,\pm q\} \\ 0, & \text{else.} \end{cases}$$
$$(36)$$

If the above function is used, an equivalent metric to (35) can be written as

$$\xi_{MLSE}[k] = \left\| \tilde{\mathbf{Y}}(k) - \sum_{m=\max[k-q,(N-N_c)/2],m\neq k}^{\min[k+q,(N+N_c)/2-1]} \mathbf{\Psi}_{imp}[k,m-k]\mathbf{X}[m] \right\|.$$
$$(37)$$

The function $\mathbf{\Psi}_{imp}[k,m]$ can be considered as the sort of non-causal time-variant impulse response at time k with the channel memory of $2q+1$, while $\mathbf{X}[m]\mid m \in \mathcal{K}$ is the symbol sequence we need to detect. The state at k is defined as

$$\sigma_k \cong (\mathbf{X}[m]\mid m \in \{\max(k-q,(N-N_c)/2),\ldots,$$
$$\min(k+q,(N+N_c)/2)-1)\}) . \quad (38)$$

Dynamic programming based on the principle of optimality, such as the Viterbi algorithm, can simplify the minimization problem (34). The minimization problem under consideration, however, requires $Q^{2(2q)}$ MLSE generalized receiver states, where Q is the constellation size. Even for small Q, the minimization problem might be computationally prohibitive. In addition, merging is the random phenomenon and it is possible that no decision is made until the end of the entire sequence. Given that the length of the sequence $\mathbf{X}[m]\mid m \in \mathcal{K}$ is N_c, this may result in N_c codeword period delay [19].

The next section describes the SDFSE generalized receiver scheme with the adaptive threshold, which mitigates both the delay and the very high complexity problem of the MLSE generalized receiver scheme.

5.2 SDFSE scheme with adaptive threshold

Among suboptimal but computationally feasible sequence estimation techniques is sequential sequence estimation. Sequential sequence estimation, which relieves the delay problem of the MLSE generalized receiver scheme, can also be combined with decisi-

on feedback scheme to further reduce complexity [20]-[23]. By assuming that we have correctly recovered the sequence

$$\sigma_{k-} \cong (\hat{\mathbf{X}}[m] \mid m \in \{\max(k-q,0.5(N-N_c),\ldots,k-1\}) \tag{39}$$

by the time we try to recover $\hat{\mathbf{X}}[k]$ an SDFSE scheme can be formulated as: for $k = (N-N_c)/2 : (N+N_c)/2 - 1$

$$\begin{cases} \hat{\sigma}_{k+} = \arg\min_{\sigma_{k+}} \xi_{SDFSE}[k], \\ \hat{\mathbf{X}}[k] \text{ is adopted and } \hat{\sigma}_{k+} \setminus \hat{\mathbf{X}}[k] \text{ is discarded} \\ k \leftarrow k+1, \end{cases} \tag{40}$$

where

$$\{k,\ldots,\min(k+q,(N+N_c)/2)-1)\}) \ ; \tag{41}$$

$$\sigma_{k+} \cong (\mathbf{X}[m] \in C_{QPSK} \times C_{QPSK} \mid m \in$$

$$\{k,\ldots,\min(k+q,(N+N_c)/2)-1)\}) \ ; \tag{41}$$

$$\xi_{SDFSE}[k] \cong \left\| \breve{\mathbf{Y}}(k) - \sum_{m=k}^{\min[k+q,(N+N_c)/2-1]} \mathbf{A}[k,m]\mathbf{X}[m] \right\| ; \tag{42}$$

$$\breve{\mathbf{Y}}(k) \cong \mathbf{Y}[k] - \sum_{m=\max[k-q,(N-N_c)/2]}^{k-1} \mathbf{A}[k,m]\mathbf{X}[m] . \tag{43}$$

Now the required number of metric calculations is $Q^{2(q+1)}$ for the estimation of symbols in a codeword.

Further complexity reduction via the adaptive threshold. Now further complexity reduction is accomplished by using the adaptive threshold. The idea of thresholding that is referred as the *T*-algorithm, was introduced to reduce the decoding complexity of the convolutional codes in [22], but no formula was proposed for selecting the threshold value. A similar idea was used in [25], in which a posteriori probabilities associated with the one-step previous states are calculated and the state is removed when the corresponding a posteriori probability is less than a threshold.

Another method to set a threshold value was proposed in [24]. In [24], the threshold value is set so that the removal probability of the correct state is less than the target error probability. In this scheme, the instantaneous *SNR* is necessary to calculate the instantaneous threshold value though. The maximal possible threshold value can be used to avoid the instantaneous threshold value calculation, which, in turn, decreases the efficiency of the threshold idea. On the other hand, in the present paper, the thresh-

old value is decided based on the time-variation degree of the channel without requiring the instantaneous *SNR* or the a posteriori probability [40].

Under the assumption that a sequence σ_{k-} was recovered correctly, a simple metric is defined

$$\xi_{simple}[k] \cong \left\| \breve{\mathbf{Y}}(k) - \mathbf{A}[k,k]\mathbf{X}[k] \right\| . \tag{44}$$

A comparison between (42) and (44) shows that the metric (42) involves a sequence σ_{k+}, while the simple metric (44) considers only $\mathbf{X}[k]$. In other words, the metric (44) considers only the intracodeword coupling effects, while the metric (42) takes into account both coupling effects. From (42) and (44), the difference between the two metrics is bounded as $\forall \mathbf{X}[k] \in C_{QPSK} \times C_{QPSK}$ and σ_{k+} with the $\mathbf{X}[k]$ we obtain

$$\left| \xi_{simple}[k] \right|_{\mathbf{X}[k]} - \xi_{SDFSE}[k] \Big|_{\sigma_{k+}} \right|$$

$$\leq \left\| \sum_{m=k+1}^{\min[k+q,(N+N_c)/2-1]} \mathbf{A}[k,m]\hat{\mathbf{X}}[m] \right\|$$

$$\leq \sqrt{2} \sum_{m=k+1}^{\min[k+q,(N+N_c)/2-1]} \left\| \mathbf{A}[k,m] \right\| \cong B[k] . \tag{45}$$

Note that the norm $\|\mathbf{X}\| = \sqrt{2}, \forall \mathbf{X}[k] \in C_{QPSK} \times C_{QPSK}$ by assuming a constellation of unit amplitude symbols. We can observe that the bound $B[k]$ is a function of the intercodeword coupling.

Let $\mathbf{X}_{subopt}[k]$ be the minimizer of the metric (44), then

$$\left| \xi_{simple}[k] \right|_{\mathbf{X}_{subopt}[k]} - \xi_{simple}[k] \Big|_{\mathbf{X}[k]} \right|$$

$$\leq \left\| \mathbf{A}[k,k](\mathbf{X}_{subopt}[k] - \mathbf{X}[k]) \right\|$$

$$\leq \left\| \mathbf{A}[k,k] \right\| \left\| \mathbf{X}_{subopt}[k] - \mathbf{X}[k] \right\| \cong C[k] . \tag{46}$$

The bound $C[k]$ is the function of the intracodeword coupling effect.

The following relationship between the above two bounds can be induced from Fig. 3

$$E\{C[k]\} = \frac{2+\sqrt{2}}{2} E\{\|\mathbf{A}[k,k]\|\} > 2E\{B[k]\}. \tag{47}$$

The above inequality again implies

$$S_k \subset \left\{ \mathbf{X}[k] \in C_{QPSK} \times C_{QPSK} \right.$$

$$\times \left| \xi_{simple}[k] \Big|_{\mathbf{X}_{subopt}[k]} - \xi_{simple}[k] \Big|_{\mathbf{X}[k]} \right| \le C[k] \Big\}, \quad (48)$$

where

$$S_k \cong \Big\{ \mathbf{X}[k] \in C_{QPSK} \times C_{QPSK}$$

$$\times \left| \xi_{simple}[k] \Big|_{\mathbf{X}_{subopt}[k]} - \xi_{simple}[k] \Big|_{\mathbf{X}[k]} \right| \le 2B[k] \Big\} . \quad (49)$$

Meanwhile, if we let $\mathbf{X}_{opt}[k]$ be the minimizer of the metric (42), the relationship between the two minimizers is derived from (33)

$$\left| \xi_{simple}[k] \Big|_{\mathbf{X}_{subopt}[k]} - \xi_{simple}[k] \Big|_{\mathbf{X}_{opt}[k]} \right| \le 2B[k] \Big\}, \quad (50)$$

which implies that $\mathbf{X}_{opt}[k] \in S_k$.

A small set of probable minimizers of the metric (42) can be chosen via the simple metric (44). This is where the idea of the adaptive threshold method is used. The smaller the bound $B[k]$ compared to $C[k]$, the smaller $|S_k|$ becomes, where $|S_k|$ is defined as the number of elements in S_k. The set S_k can be regarded as the candidate set of $\mathbf{X}[k]$. After the selection of the candidates of $\mathbf{X}[k]$, which requires Q^2 metric calculations of $\xi_{simple}[k]$, $S_k \cdot Q^2$ metric calculations are necessary to find the minimizer of $\xi_{SDFSE}[k]$. In other words, the intracodeword coupling effects are first considered for the estimation of the transmitted symbols and the intercodeword coupling effects are considered only when there are more than one contender. Note that when the large q needs to be considered, the idea of the threshold can be further exploited by defining another simple metric including a few the intercodeword coupling effects. We also note that the adaptive threshold decreases not only the number of metric calculations but also the complexity of each metric calculation via (44).

5.3 AESE scheme

To further reduce the average complexity of the SDFSE generalized scheme with the adaptive threshold, the AESE generalized receiver scheme is proposed in this section. The basic idea is that when the instantaneous channel variation is small, $\|\mathbf{C}_{INTRA}[k]\|$ for each $k \in \mathcal{K}$ is smaller than the threshold T_{AESE}, the simple Alamouti decoding generalized receiver scheme is used. On the other hand, the SDFSE generalized receiver scheme with the adaptive threshold is used to mitigate the performance degradation when the instantaneous channel variation is large.

Consequently, $\|\mathbf{C}_{INTRA}[k]\|$ is larger than the threshold. The block diagram of the proposed adaptive effort with the generalized receiver is presented in Fig. 5. This scheme is based on the observation that the high Doppler frequency implies the statistical fast fading channel but it does not necessarily mean significant instantaneous channel variation. To quantify the effectiveness of the proposed AESE generalized receiver scheme, we define the following probability that an instantaneous channel variation is significant and, consequently, an Alamouti codeword is estimated via the SDFSE generalized receiver scheme with the adaptive threshold [41]

$$P_{AESE} \cong P(\|\mathbf{C}_{INTRA}[k,k]\| > T_{AESE}) . \quad (51)$$

The trade off between complexity and performance can be made via T_{AESE} in the AESE generalized receiver scheme. Larger T_{AESE} means that more symbols are estimated via the simple Alamouti decoding generalized receiver. Thus, a complexity can be reduced by using larger T_{AESE} but the performance will be degraded at the same time.

5.4 Computational complexity

In this section, the computational complexity of various schemes is compared. The required number of metric calculations for the proposed schemes is summarized in Table I. Since we are considering $q = 1$, the number of metric calculations required in SDFSE generalized receiver with the adaptive threshold is $(1 + |\overline{S}_k|)Q^2$, where

$$|\overline{S}_k| = \sum_{i=2}^{Q^2} iP(|\overline{S}_k| = i) . \quad (52)$$

In the process of decoding N_c Alamouti codewords, $4N_c(1 + |\overline{S}_k|)Q^2$ multiplications are required per Alamouti codeword period. The average complexity can be further reduced via the adaptive effort scheme based on the generalized receiver with only negligible performance degradation.

To assess the complexity of the time-domain MMSE approach, the MMSE generalized receiver scheme design procedure as well as the MMSE filtering procedure needs to be included. In the filter design procedure, the correlation matrix $\mathbf{R}_{yy}$ in [12, Section IVB] is constructed first with the size $2N \times 2N$ for the two-transmit and one-received antenna systems, requiring $8N^3$ multiplications. Using the sparse structure of the corresponding matrices, the comple-

xity is lowered to $4N^2 \times 2L$, where L is the number of multipaths for each channel. Then, the inverse of the correlation matrix is calculated that requires $8N^3$ multiplications. Finally, a time-variant filter is designed as described in Section 5.2 ($8N^3$ multiplications). In the filtering process, $4N^2$ multiplications are required since the length of the filter is $2N$. Therefore, roughly $3 \times 8N^3 + 4N^2$ multiplications are required per Alamouti codeword period. The low rank approximation of the correlation matrix that was used in [42] can be adopted to reduce complexity in the filter design process. Unlike in [42], however, a low rank approximation is necessary per codeword period. It seems that the computationally expensive singular value decomposition in the approximation process does not reduce the complexity dramatically.

Since we are considering the parameters $N = 128$ and $Q = 4$, the complexity of the proposed SDFSE generalized receiver with the adaptive threshold is much lower in comparison with the MMSE generalized receiver approach. Since the MMSE generalized receiver scheme complexity does not depend on the constellation size Q, the relative complexity of the proposed schemes grows as larger constellations are used. But under the harsh channel environment we are considering here, the small signal constellation may be used to achieve a proper error performance.
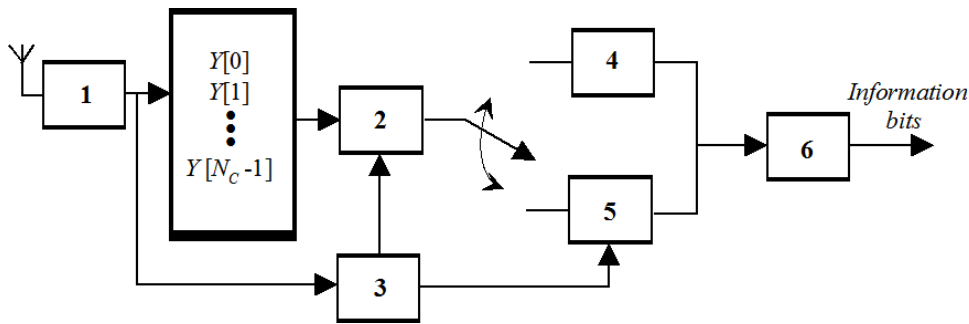

Fig. 5. Block diagram of the proposed adaptive effort generalized receiver. When the instantaneous channel time variation is significant the SDPSE with the adaptive threshold is used, and when it is not significant the simple Alamouti decoding is used: 1- fast Fourier transform; 2 – generalized receiver; 3 – channel estimation; 4 – Alamouti decoding; 5 – SDFSE with the adaptive threshold; 6 – QPSK demodulator.

Table I. Required number of metric calculations for an Alamouti codeword estimation in various symbol estimation schemes based on the generalized receiver.

Decoding scheme	Required number of metric calculations
Alamouti decoding scheme	$2 \times Q^2$
SDFSE	$Q^{2(q+1)}$
SDFSE with the adaptive threshold	$Q^2 + \mid \bar{S}_k \mid Q^{2q}$
AESE	$P_{AESE}(Q^2 + \mid \bar{S}_k \mid Q^{2q}) + (1 - P_{AESE})2Q$

6 Simulation Results

In this section, the error performance and complexity of the following schemes are compared via simulation: the Alamouti decoding generalized receiver scheme, the SDFSE generalized receiver scheme with the adaptive threshold, the AESE generalized receiver scheme, the STBC generalized receiver scheme, and the MMSE generalized receiver approach. The simulation scenario is the same as in Section 4.3. We consider only the higher Doppler frequency of 297 Hz resulting in the normalized Doppler frequency of $f_D(N + D)T_s = 0.12$. Unlike in Section

4.3, we consider both cases with and without ideal channel state information at the receiver. Considered values for T_{AESE} in the AESE generalized receiver scheme are 0.3 and 0.4. Exact noise power is assumed to be available for the MMSE generalized receiver approach.

The *BER* performance as a function of the *SNR* for various decoding schemes is presented in Fig. 6 when the ideal channel state information is assumed. The time-domain MMSE generalized receiver approach shows the best performance. The performance of the proposed SDFSE generalized receiver with the adaptive threshold falls between the Alamouti decoding generalized receiver performance and that of the MMSE generalized receiver approach. It can be observed that as the parameter q increases in the proposed SDFSE generalized receiver with the adaptive threshold, the performance approaches that of the MMSE generalized receiver. For the *SNR* range from 5 to 25 dB, the proposed SDFSE generalized receiver with the adaptive threshold $(q = 2)$ shows almost the same performance as that of the MMSE generalized receiver. When the *SNR* is as high as 30 dB, there exists a performance difference though. The performance gap seems to be due to the fact that the MMSE generalized approach considers the intercodeword coupling from all subchannels while the SDFSE generalized receiver with the adaptive threshold considers intercodeword coupling from only $2q$ adjacent subchannels. The performance gap suggests that, as the *SNR* gets higher, more subchannels need to be considered from which the intercodeword coupling is caused.
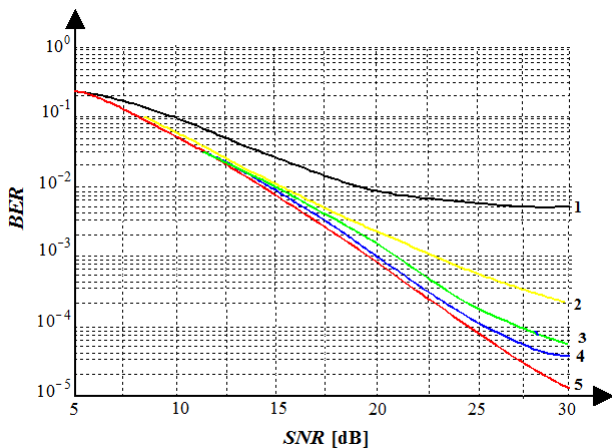

Fig. 6. *BER* performance (perfect channel state information) of the Alamouti decoding (1), proposed SDFSE with the adaptive threshold (2- $q = 0$, 3- $q = 1$, 4- $q = 2$), and time-domain MMSE schemes (5) based on the generalized receiver.

The *BER* performance when the channel state information is estimated via the channel estimation technique discussed in [12] is presented in Fig. 7. The performance degradation due to channel estimation error can be observed. The decoding schemes react differently to the channel estimation error. The error performance of the Alamouti decoding generalized receiver and the SDFSE generalized receiver with the adaptive threshold $(q = 0)$ is almost identical as when the ideal channel state information is assumed. With channel estimation error, however, the SDFSE generalized receiver with the adaptive threshold $(q = 2)$ shows almost the same performance as that of the SDFSE generalized receiver with the adaptive threshold $(q = 1)$, which suggests that the intercodeword coupling $\mathbf{A}[k, k+2]$ is more susceptible to channel state information estimation error than $\mathbf{A}[k, k]$ and $\mathbf{A}[k, k+1]$ are. The MMSE generalized receiver approach shows the most significant performance gap between the ideal and estimated channel state information.
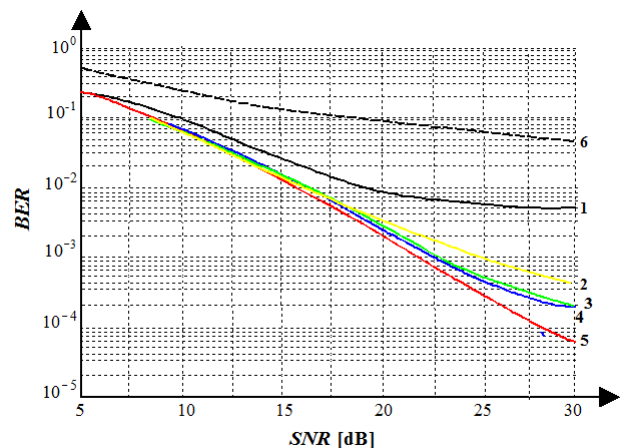

Fig. 7. *BER* performance (perfect channel state information) of the Alamouti decoding (1), proposed SDFSE with the adaptive threshold (2- $q = 0$, 3- $q = 1$, 4- $q = 2$), time-domain MMSE (5) schemes based on the generalized receiver, and differential STBC scheme (no channel state information).

The *BER* performance shown in Fig. 7 suggests that with the channel state information estimation error, large q does not have to be adopted in the SDFSE generalized receiver with the adaptive threshold. It shows also that with the channel state information estimated the proposed SDFSE generalized receiver with the adaptive threshold $(q = 1)$ demonstrates a negligible performance degradation compared with the MMSE generalized receiver approach.

Figure 7 also presents the performance of the differential scheme [18]. Although the differential

scheme eliminates the need for the channel state information, which is more beneficial when the channel parameters change very fast, its performance loss due to the non-quasistatic channels is much more severe than the performance less of other coherent schemes due to the channel state information estimation error. It seems that the performance loss is caused by the strict assumption of the differential scheme that the channels do not change over two Alamouti codeword periods, i.e., four OFDM symbol periods. Note that the Alamouti decoding generalized receiver scheme assumes that the channel parameters do not change over only two OFDM symbol periods.
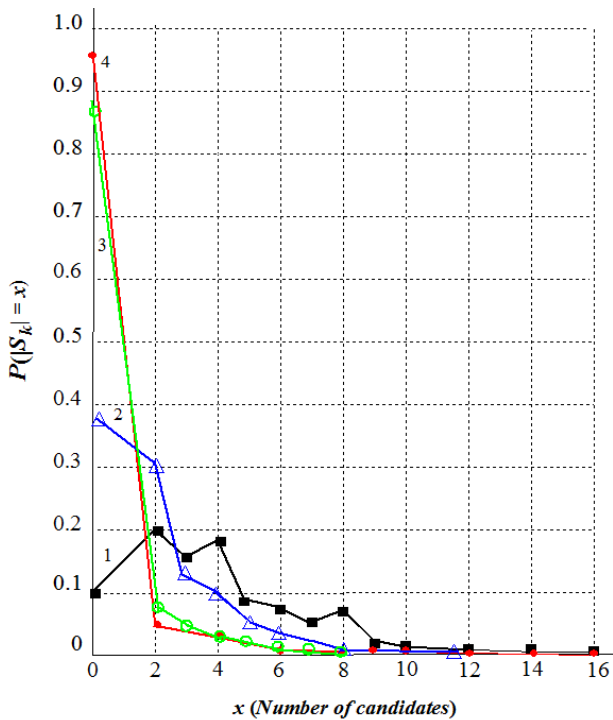

Fig. 8. Number of candidates in the proposed SDFSE generalized receiver with the adaptive threshold $(q=1)$ for various *SNR* values:

1 - *SNR* = 5 dB; 2- *SNR* = 10 dB; 3- *SNR* = 20 dB; 4- *SNR* = 30 dB. Estimated channel state information is used.

The probability of the number of candidates in the SDFSE generalized receiver with the adaptive threshold scheme $(q=1)$ is presented in Fig. 8. It can be observed that more candidates are selected when the *SNR* is low. This is because that more constellation points satisfy the constraint (49) due to dominant background noise. As the *SNR* increases, the number of candidates significantly decreases. When the *SNR* is 20 dB, only one candidate is selected with the probability of 0.9. The corresponding $|\overline{S}_k| =$

0.2; hence, the complexity of the SDFSE generalized receiver with the adaptive threshold is $N_c \times 1.2 \times Q^2 \times 4$ multiplications per the Alamouti codeword period. The complexity of the proposed approach is much lower than $2 \times 8N^3 + 4N^2$ of the MMSE generalized receiver approach when a moderate Q is assumed. The complexity ratio of the proposed receiver to the MMSE generalized receiver approach is

approximately $5Q^2 / 24N^2$.

The performance of the SDFSE generalized receiver with the adaptive threshold $(q=1)$, AESE generalized receiver with $T_{AESE} = 0.3; 0.4$, and the MMSE generalized receiver approaches are presented in Fig. 9. As can been seen from the Fig. 9, the AESE generalized receiver scheme shows negligible performance degradation compared with SDFSE generalized receiver with the adaptive threshold $(q=1)$ scheme when the threshold value $T_{AESE} = 0.3$. Therefore, about 42% of transmitted signals are estimated via the Alamouti decoding generalized receiver scheme even when the Doppler frequency is as high 297 Hz, if $T_{AESE} = 0.3$. Although the higher T_{AESE} can be used to further decrease the complexity, when $T_{AESE} = 0.4$ the probability goes down to 35%, there exist significant performance gaps. Therefore, it can be concluded that the proposed AESE generalized receiver scheme with appropriate T_{AESE} is the attractive receiver for the Alamouti coded OFDM systems in the fast fading channels.
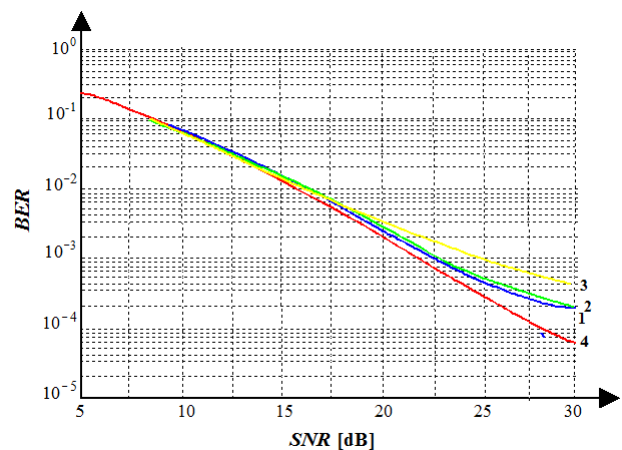

Fig. 9. *BER* performance (estimated channel state information) of: 1 - SDFSE generalized receiver with the adaptive threshold $(q=1)$; 2 - AESE generalized receiver with $T_{AESE} = 0.3$; 3 - AESE with generalized receiver $T_{AESE} = 0.4$; 4 - time-domain

MMSE generalized receiver scheme.

7 Conclusions

In Alamouti coded OFDM systems, the time variation of channel causes both the intercodeword couplings, which significantly degrade the performance of the Alamouti decoding generalized receiver performance. We showed that the performance degradation can be mitigated by the SDFSE generalized receiver scheme with the adaptive threshold at a much lower complexity when compared with the previous MMSE generalized receiver approach and a small constellation is assumed, exploiting the relative significance of the two couplings. It was also shown that the performance difference between the MMSE generalized receiver and the SDFSE generalized receiver with the adaptive threshold schemes becomes smaller when the channel state information estimation error is taken into account. When the very large constellation and small FFT size are adopted, the SDFSE generalized receiver with the adaptive threshold scheme may require higher complexity was achieved based on the observation that the high Doppler frequency does not necessarily mean significant instantaneous channel variation all the time, which motivated the development of the adaptive effort receiver. The simulation demonstrated the efficacy of the proposed SDFSE generalized receiver with the adaptive threshold and AESE generalized receiver schemes.

References
[1] V. Tarokh, N. Seshadri, and A.R. Calderbank, Space-time codes for high data rate wireless communication: performance criterion and code construction//*IEEE Transactions on Information Theory.*1998, Vol. 44, No.2, pp. 744-765.

[2] A.F. Naguib, N. Seshadri, and A.R. Calderbank, Increasing data rate over wireless channel//*IEEE Signal Processing Magazine.* 2000, Vol. 17, No. 3, pp.76-92.

[3] V. Tarokh, H. Jafarkhani, and A.R. Caldebank, Space-time block codes from orthogonal designs//*IEEE Transactions on Information Theory.* 1999, Vol.45, No. 5, pp. 1456-1467.

[4] V. Tarokh, H. Jafarkhani, and A.R. Caldebank, Space-time block coding for wireless communications: Performance results//*IEEE Journal on Selected Areas on Communications.* 1999, Vol. 17, No. 3, pp. 451-460.

[5] X. Li, N. Luo, G. Yue, and C.Yin, A squariung method to simplify the decoding of orthogonal space-time block codes//*IEEE Transactions on Communications*. 2001, Vol. 49, No. 10, pp.

1700-1703.

[6] S.M. Alamouti, A simple transmit diversity technique for wireless communications//*IEEE Journal on Selected Areas on Communications.* 1998, Vol. 16, No. 10, pp. 1451-1458.

[7] M. Hoseinzade, K. Mohamedpour, S. Medhi Hosseini Andargoli, Decision feedback channel estimation for Alamouti coded OFDM systems// *International Journal of Information & Communication Technology Research.* 2012, Vol. 4, Issue 3, pp.1-11.

[8] R. Bhadada, R. Taparia, Performance analysis of Alamouti code MIMO OFDM systems for error control and IQ impairments//*Communications on Applied Electronics.* 2015, Vol. 1, No. 2, pp.14-17.

[9] M.A. Youssefi, N. Bounouader, Z. Guennoun, J.E. Abdadi, Adaptive switching between space-time and space-frequency block coded OFDM systems in Rayleigh fading channel//*International Journal of Communications, Network and System Sciences.* 2013, Vol. 6, No. 6, Article ID:3230,8 pages;doi:10.4236/ijcns.2013.66034

[10] B.-S. Kim, K.H. Choi, Over-sampling effect in distributed Alamouti coded OFDM with frequency offset//*IET Communications.* 2016, Vol. 10, Issue 17, pp. 2344-2351.

[11] H.A. Bakir, F. Debhat, and F.T. Bendimerad, Performance enhancement of OSTBC applied OFDM modulation for wireless communication systems//*Journal of Applied Sciences*. 2016, Vol.16, pp. 419-428; doi:10.3923/jas.2016.419.428

[12] A. Stamoulis, S.N. Diggavi, N. Al-Dhahir, Intercarrier interference in MIMO OFDM//*IEEE Transactions on Signal Processing.* 2002, Vol. 50, No. 10, pp. 2451-2464.

[13] Z. Liu, X. Ma, G.B. Giannakis, Space-time coding and Kalman filtering for time-selective fading channels//*IEEE Transactions on Communications.*2002, Vol. 50, No. 2, pp. 183-186.

[14] B.S. Kim, D. Na, K.H. Choi, Partial ML detection for frequency-asynchronous distributed Alamouti-coded (FADAC) OFDM//*Wireless Communications and Mobile Computing. Special Issue: Antenna Design Techniques for 5G Mobile Communications*. 2019, Volume 2019, Article ID:4319802;doi:10/1155/2019/4319802

[15] B.S. Kim, K.H.Choi, Iterative detection for frequency-asynchronous distributed Alamouti-coded (FADAC) OFDM//*EURASIP Journal on Wireless Communications and Networking.* 2017,39(2017);doi:10.1186/S13638-017-0819-1

[16] I.B. Djordjevich, L. Xu, T. Wang, Alamouti-ty-

pe polarization-time coding in coded-modulation schemes with coherent detection//*Optic Express*. 2008, Vol. 16, Issue 18,pp.14163-14172.

[17] K. Choi, Intercarrier interference free Alamouti coded OFDM for cooperative systems with frequency offsets in non-selective fading environments//*IET Communications.* 2011, Vol. 5, Issue 15, pp.2125-2129.

[18] S.N. Figgavi, N. Al-Dhahir, A Stamoulis, A.R. Calderbank, Diferential space-time coding for frequency-selective channels//*IEEE Communications Letters*. 2002, Vol.6, No.6, pp.253-255.

[19] J.F. Hayes, The Viterbi algorithm applied to digital data transmission//*IEEE Communications Magazine*. 2002, Vol. 40, No. 5, pp. 26-32

[20] A. Duel-Hallen, C. Heegard, Delayed decision-feedback sequence estimation//*IEEE Transactions on Communications*. 1989, Vol. 37, No. 5, pp. 428-436.

[21] W. Younis, N. Al-Dhahir, Joint prefiltering and MLSE equalization of space-time-coded transmissions over frequency-selective channels//*IEEE Transactions on Vehicular Technology*. 2002, Vol. 51, No. 1, pp. 144-154.

[22] S.J. Simmons, Breadth-first trellis decoding with adaptive effort////*IEEE Transactions on Communications*. 1989, Vol. 37, No. 5, pp. 428-436.

[23] W. Gerstacker, R. Schober, Equalization concepts for EDGE//*IEEE Transactions on Wireless Communications.* 2002, Vol.1, No. 1, pp. 190-199.

[24] H. Zamiri-Jafarian, S. Pasupathy, Complexity reduction of the MLSD/MLSDE receiver using the adaptive state allocation algorithm// *IEEE Transactions on Wireless Communications.* 2002, Vol.1, No. 1, pp. 190-199.

[25] J.P. Seymour, M.P. Fitz, Near-optimal symbol-by-symbol detection schemes for flat Rayleigh fading//*IEEE Transactions on Communications* 2002, Vol.1, No. 2/3/4, pp. 1525-1533.

[26] W. Jeon, K. Chang, Y. Cho, An equalization technique for orthogonal frequency division multiplexing systems in time-variant multipath channels// *IEEE Transactions on Communications.* 1999, Vol.47, No. 1, pp. 27-32.

[27] V. Tuzlukov, A new approach to signal detection theory. *Digital Signal Processing: Review Journal*. 1998, Vol.8, No. 3, pp.166–184.

[28] V. Tuzlukov, *Signal Detection Theory*. Springer-Verlag, New York, USA, 2001, 746 pp.

[29] V. Tuzlukov, *Signal Processing Noise*. CRC Press, Boca Raton, London, New York, Washington, D.C., USA, 2002, 692 pp.

[30] M. Maximov, Joint correlation of fluctuative noise at outputs of frequency filters. *Radio Engineering.* 1956, No. 9, pp. 28–38.

[31] Y. Chernyak, Joint correlation of noise voltage at outputs of amplifiers with no overlapping responses. *Radio Physics and Electronics.* 1960, No. 4, pp. 551–561.

[32] Shbat, M., Tuzlukov, V.P. Definition of adaptive detection threshold under employment of the generalized detector in radar sensor systems. *IET Signal Processing.* 2014, Vol. 8, Issue 6, pp. 622–632.

[33] Tuzlukov, V.P. DS-CDMA downlink systems with fading channel employing the generalized. *Digital Signal Processing.* 2011. Vol. 21, No. 6, pp. 725–733.

[34] *Communication Systems: New Research*, Editor: Vyacheslav Tuzlukov, NOVA Science Publishers, Inc., New York, USA, 2013, 423 pp.

[35] Shbat, M., Tuzlukov, V.P. Primary signal detection algorithms for spectrum sensing at low SNR over fading channels in cognitive radio. *Digital Signal Processing* (2019). https://doi.org/10.1016/j.dsp. 2019.07.16. *Digital Signal Processing.* 2019, Vol. 93, No. 5, pp. 187- 207.

[36] V. Tuzlukov, Signal processing by generalized receiver in wireless communications systems over fading channels," Chapter 2 in *Advances in Signal Processing*. IFSA Publishing Corp. Barcelona, Spain. 2021. pp. 55-111.

[37] V. Tuzlukov, Interference Cancellation for MIMO Systems Employing the Generalized Receiver with High Spectral Efficiency". *WSEAS Transactions on Signal Processing.* 2021, Vol. 17, Article #1, pp. 1-15.

[38] M. Shbat and V. Tuzlukov, SNR wall effect alleviation by generalized detector employment in cognitive radio networks. *Sensors*, 2015, 15 (7), pp.16105-16135;doi:10.3390/s150716105.

[39] V. Tuzlukov, Signal processing by generalized detector in DS-CDMA wireless communication systems with frequency-selective channels. *Circuits, Systems, and Signal Processing*. Published on-line on February 2, 2011, doi:10.1007/ s00034-011-9273-1; 2011, Vol.30, No.6, pp. 1197–1230.

[40] M. Shbat, V. Tuzlukov, Generalized detector as a spectrum sensor in cognitive radio networks, "*Radioengineering* , 2015, Vol. 24, No. 2, pp. 558–571.

[41] W.C. Jakes, *Microwave Mobile Communications.* New York: Wiley, 1974.

[42] Y. Choi, P.J. Voltz, F.A. Cassara, On channel estimation and detection for multicarrier signals in fast and selective Rayleigh fading channels//*IEEE Transactions on Communications.*

Dr. Vyacheslav Tuzlukov received the MSc and PhD degrees in radio physics from the Belarusian State University, Minsk, Belarus in 1976 and 1990, respectively, and DSc degree in radio physics from the Kotelnikov Institute of Radioengineering and Electronics of Russian Academy of Sciences in 1995. Starting from 1995 and till 1998 Dr. Tuzlukov was a Visiting Professor at the University of San-Diego, San-Diego, California, USA. In 1998 Dr. Tuzlukov relocated to Adelaide, South Australia, where he served as a Visiting Professor at the University of Adelaide till 2000. From 2000 to 2002 he was a Visiting Professor at the University of Aizu, Aizu-Wakamatsu City, Fukushima, Japan and from 2003 to 2007 served as an Invited Professor at the Ajou University, Suwon, South Korea, within the Department of Electrical and Computer Engineering. Starting from March 2008 to February 2009 he joined as a Full Professor at the Yeungnam University, Gyeonsang, South Korea within the School of Electronic Engineering, Communication Engineering, and Computer Science. Starting from March 1, 2009 Dr. Tuzlukov served as Full Professor and Director of Signal Processing Lab at the Department of Communication and Information Technologies, School of Electronics Engineering, College of IT Engineering, Kyungpook National University, Daegu, South Korea. Currently, Dr. Tuzlukov is the Head of Department of Technical Exploitation of Aviation and Radio Engineering Equipment, Belarusian State Academy of Aviation, Minsk, Belarus. His research emphasis is on signal processing in radar, wireless communications, wireless sensor networks, remote sensing, sonar, satellite communications, mobile communications, and other signal processing systems. He is the author over 280 journal and conference papers, seventeenth books in signal processing published by Springer-Verlag and CRC Press. Some of them are *Signal Detection Theory* (2001), *Signal Processing Noise* (2002), *Signal and Image Processing in Navigational Systems* (2005)*, Signal Processing in Radar Systems* (2012), Editor of the book *Communication Systems: New Research* (2013), Nova Science Publishers, Inc, USA, and has also contributed Chapters "Underwater Acoustical Signal Processing" and "Satellite Communications Systems: Applications" to *Electrical Engineering Handbook: 3rd Edition*, 2005, CRC Press; "Generalized Approach to Signal Processing in Wireless Communications: The Main Aspects and Some Examples" to *Wireless Communications and Networks: Recent Advances*, InTech, 2012; "Radar Sensor Detectors for Vehicle Safety Systems" to *Electrical and Hybrid Vehicles: Advanced Systems, Automotive Technologies, and Environmental and Social Implications*, Nova Science Publishers, Inc., USA, 2014; "Wireless Communications: Generalized Approach to Signal Processing" and "Radio Resource Management and Femtocell Employment in LTE Networks", to *Communication Systems: New Research*, Nova Science Publishers, Inc., USA, 2013; "Radar Sensor Detectors for Vehicle Safety Systems" to *Autonomous Vehicles: Intelligent Transport Systems and Automotive Technologies*, Publishing House, University of Pitesti, Romania, 2013; "Radar Sensor Detectors for Vehicle Safety Systems," to *Autonomous Vehicles: Intelligent Transport Systems and Smart Technologies*, Nova Science Publishers, Inc., New York, USA, 2014; "Signal Processing by Generalized Receiver in DS-CDMA Wireless Communication Systems," to *Contemporary Issues in Wireless Communications*. INTECH, CROATIA, 2014; "Detection of Spatially Distributed Signals by Generalized Receiver Using Radar Sensor Array in Wireless Communications," to *Advances in Communications and Media Research*. NOVA Science Publishers, Inc., New York, USA, 2015; "Signal Processing by Generalized Receiver in Wireless Communication Systems over Fading Channels" to *Advances in Signal Processing*. IFSA Publishing Corp. Barcelona, Spain. 2021; "Generalized Receiver: Signal Processing in DS-CDMA Wireless Communication Systems over Fading Channels" to *Book Title: Human Assisted Intelligent Computing: Modelling, Simulations and Its Applications*. IOP Publishing, Bristol, United Kingdom, 2022. He participates as the General Chair, Keynote Speaker, Plenary Lecturer, Chair of Sessions, Tutorial Instructor and organizes Special Sections at the major International Conferences and Symposia on signal processing.

Dr. Tuzlukov was highly recommended by U.S. experts of Defence Research and Engineering (DDR& E) of the United States Department of Defence as a recognized expert in the field of humanitarian demining and minefield sensing technologies and had been awarded by Special Prize of the United States Department of Defence in 1999 Dr. Tuzlukov is distinguished as one of the leading achievers from around the world by Marquis Who's Who and his name and biography have been included in the Who's Who in the World, 2006-2013; Who's Who in World, 25th Silver Anniversary Edition, 2008, Marquis Publisher, NJ, USA; Who's Who in Science and Engineering, 2006-2012 and Who's Who in Science and Engineering, 10th Anniversary Edition, 2008-2009, Marquis Publisher, NJ, USA; 2009-2010 Princeton Premier Business Leaders and Professionals Honours Edition, Princeton Premier Publisher, NY, USA; 2009 Strathmore's Who's Who Edition, Strathmore's Who's Who Publisher, NY, USA; 2009 Presidental Who's Who Edition, Presidental Who's Who Publisher, NY, USA; Who's Who among Executives and Professionals, 2010 Edition, Marquis Publisher, NJ, USA; Who's Who in Asia 2012, 2nd Edition, Marquis Publisher, NJ, USA; Top 100 Executives of 2013 Magazine, Super Network Publisher, New York, USA, 2013; 2013/2014 Edition of the Global Professional Network, Business Network Publisher, New York, USA, 2013; 2013/2014 Edition of the Who's Who Network Online, Business Network Publisher, New York, USA, 2014; Online Professional Gateway, 2014 Edition, Business Netw-

ork Publisher, New York, USA, 2014; 2014 Worldwide Who's Who", Marquis Publisher, NJ, USA; 2015 Strathmore Professional Biographies, Strathmore's Who's Who Publisher, NY, USA; Who's Who in World, 2015, Marquis Publisher, NJ, USA; 2015-2016 Membership in Exclusive Top 100 network of professionals in the world, NY, USA, 2015; 2015 Who's Who of Executives and Professionals Honors Edition, Marquis Publisher, NJ, USA; Worldwide Who's Who – Top 100 Business Networking, San Diego, CA, USA, 2015.

Phone: +375173453283; Email: slava.tuzlukov@mail.ru